Publication II

Mika Karjalainen. 2007. Geocoding of synthetic aperture radar images using digital vector maps. IEEE Geoscience and Remote Sensing Letters, volume 4, number 4, pages 616-620.

Geocoding of Synthetic Aperture Radar Images Using Digital Vector Maps

Mika Karjalainen

***Abstract*—In this letter, a possible approach to automate synthetic aperture radar (SAR) geocoding (or to automatically refine the existing one) is presented. The procedure is based on edge detection, where ground control lines obtained from digital vector maps are located in the SAR images. In geocoding, affine, projective, and rigorous SAR sensor transformation models can be used. According to the experiments, the procedure seems to be accurate and reliable as long as the initial values of the geocoding transformation model are accurate enough. The procedure copes well with displacements of about ten pixels on SAR images, but good results have been obtained in cases of even larger displacements. According to the well-defined checkpoints, the resulting geocoding accuracies for test images were around a few pixels. When the rigorous SAR sensor model was used, the accuracies were less than two pixels in most cases.**

***Index Terms*—Image edge analysis, image orientation analysis, synthetic aperture radar (SAR).**

I. Introduction

THE GOAL of geocoding is to relate any remote sensing image to the real-world coordinate system. Once images are geocoded, it is then possible to overlay images that are taken at different times from different perspectives and with different sensors to carry out, e.g., change detection, mapping, map updating, image mosaicing, or stereo plotting [1]. In the process of geocoding, one would need, first, ground control features such as ground control points (GCPs) and their corresponding locations on the images and, second, a mathematical model to transform the coordinates between the object and the image coordinate systems. Hence, the geocoding process basically consists of the following fundamental problems: 1) selecting or designing an appropriate mathematical transformation model, which describes the imaging geometry of the sensor; 2) localization of the ground control features on the images; and 3) calculation of the parameters of the transformation model.

Considering their parameters, the transformation models can be divided into three categories: 1) nonphysical models; 2) rigorous models; and 3) hybrid models. Nonphysical models are able to transform coordinates between the object and the image space, but it is usually not possible to directly perceive the location, movement, or pose of the sensor in the object coordinate system [2]. Affine and projective transformations are typical examples of nonphysical transformation models that are used in the geocoding of synthetic aperture radar (SAR) images.

In rigorous transformations, physical parameters are used to model the propagation of the electromagnetic radiation between the object and the image coordinate systems as exactly as possible. For example, in the case of aerial imagery, the perspective camera model is a rigorous sensor model. On the other hand, in the case of SAR geocoding, the rigorous model is commonly defined using Doppler and range equations, which were first introduced in [3]. The rigorous SAR sensor model is presented in more detail later in this letter.

Hybrid models are combinations of nonphysical and rigorous models. Typically, hybrid models are exploited in situations where the sensor geometry is partly unknown, but can be replaced with a nonphysical model using some physical constraints. For example, a hybrid model for the SAR images can be based on a simple polynomial model, where the displacements caused by the terrain topography are corrected using the digital elevation model and *a priori* information about the imaging geometry of the SAR sensor [4].

To retrieve the geocoding transformation parameters of a SAR image, some 3-D GCPs and their image coordinates are needed. It is then possible to solve the transformation parameters of the rigorous SAR sensor model using the range and Doppler equations and the least squares adjustment. An alternative approach to using GCPs is direct geocoding, which uses the geographic positioning system (GPS) and the inertial measurement unit (IMU) to directly retrieve the parameters. However, calculating the object space coordinates is basically extrapolation. Hence, from the reliability point of view, the use of some ground control is still necessary.

The use of GCPs requires that there are some clearly distinguishable point-type features in the images (preferably signalized points), whose 3-D coordinates in the object space are known. In the case of SAR images, the localization of the GCPs can be rather difficult. Therefore, the GCPs are typically digitized manually, where topographical maps (paper or digital maps) and images are compared with each other to find similar point-type features. The key to the automation of the geocoding process is the automation of the ground control localization and measurement. One possible solution is to use image correlation techniques, where previously geocoded or simulated SAR images are used as ground control. In favorable conditions, image correlation provides excellent results, and even subpixel geocoding accuracies have been achieved for Radarsat-1, ERS, and Envisat satellite SAR images [5]. An alternative approach to image correlation is the use of control features, i.e., points, lines, or polygons. It is well known that it may be hard to

Manuscript received September 1, 2006; revised May 6, 2007.

The author is with the Department of Remote Sensing and Photogrammetry, Finnish Geodetic Institute, Masala 02431, Finland (e-mail: mika.karjalainen@fgi.fi).

Color versions of one or more of the figures in this paper are available online at http://ieeexplore.ieee.org.

Digital Object Identifier 10.1109/LGRS.2007.903077

locate point-type features (other than dihedral corner reflectors), which are well definable on the images. Usually, the best point-type features are road intersections, bridges, buildings, small islands, or lakes. However, an automatic measurement of these point features is apparently difficult; hence, the use of other types of control features, namely, lines and polygons, has been studied in recent years. The idea of using mapping entities as control features was first proposed in [6], but similar approaches have also been used in the field of computer vision [7]. The line type of control features can also be used in SAR geocoding. However, due to the speckle, the robust detection of lines without prior information is rather complicated [8], [9]. For example, road networks that are extracted from a geographic information system can be used to create GCPs [10]. Ground control features can also be derived from other types of geocoded images, such as in [11], where SAR and SPOT images were progressively coregistered with each other using first points, second patches, and, finally, linear features. Another good example of the applicability of line features in multisource image geocoding was presented in [12]. A detailed review of the benefits of the lines as control features is presented in [13].

This letter introduces a method to automatically determine or refine the geocoding parameters of the SAR images using existing digital vector maps. Line-type control features, i.e., ground control lines (GCLs), are used to create GCPs, which are needed in the calculation of the parameters of the transformation model. The automatic measurement of the GCLs is based on edge detection, which tries to locate the projected GCLs from the SAR images. The proposed idea is similar to the edge detection approach that was presented in [11]; however, in this case, a rigorous SAR sensor model is used, and the exploitation of edge pixels is different, because there are no exact point-to-point correspondences.

II. Methodology

A. Applied SAR Geocoding Transformation Models

Three different transformation models were applied in this study: 1) affine; 2) projective transformation; and 3) rigorous SAR sensor. Because of their simplicity, the mathematical equations of the affine and projective transformation models are not presented here in detail; however, it should be noted that they are both coordinate transformations from plane to plane; therefore, they are applicable for SAR images only if the target area is flat. On the other hand, the rigorous SAR sensor model takes into account terrain topography and is able to transform coordinates between 3-D object and 2-D image coordinate systems. The rigorous SAR sensor model is based on the Doppler and range equations [3], which are defined as follows:

$$f_{\mathrm{DC}} = 2\left(\vec{\dot{s}} - \vec{\dot{p}}\right) \cdot (\vec{s} - \vec{p})/\lambda |\vec{s} - \vec{p}| \tag{1}$$

$$R = |\vec{s} - \vec{p}| \tag{2}$$

where λ is the wavelength, f_{DC} is the Doppler frequency shift, R is the measured range by the SAR sensor, $\vec{p}$ and $\vec{\dot{p}}$ are the position and velocity vectors of a ground point, respectively, and $\vec{s}$ and $\vec{\dot{s}}$ are the position and velocity vectors of the SAR sensor, respectively. Using these equations, it is possible to carry out coordinate transformations between the object and the image coordinate systems. The unknown parameters in the range and Doppler equation system are the location and velocity of the SAR sensor as a function of time. When some GCPs and their corresponding image coordinates are available, it is possible to solve the unknown parameters using the least squares adjustment. When GCLs are used, there are no exact point-to-point correspondences. Therefore, it is necessary to produce the so-called virtual GCPs, which are explained in more detail in Section II-C. The solved geocoding parameters approximately model the trajectory of the sensor in the coordinate systems that are defined by the GCPs. For spaceborne SAR images, a polynomial function can be used to model the sensor trajectory. In general, the geocoding procedure of satellite SAR images is presented in more detail in [14].

In this letter, one simplification has been applied to the general case of the satellite SAR sensor model, where a geocentric Cartesian coordinate system is used. Here, the trajectory of the SAR sensor is directly modeled in the local map coordinate system, which is defined by the ground control. Since the map coordinate system is a plane that is tangential to the Earth's ellipsoid, the distances measured by the SAR sensor (i.e., the ground range values) have to be corrected to the map plane by taking into account the Earth's curvature. When focused SAR images are used, the measured ground range values can be corrected to the tangential map plane with the following formula:

$$R_{\mathrm{map}} = \sqrt{R_{\mathrm{near}}^2 + GR_{\mathrm{map}}^2 - 2R_{\mathrm{near}}GR_{\mathrm{map}}\cos(i_{\mathrm{near}} + 90)} \tag{3}$$

where R_{map} is the distance from the SAR sensor to a given point on the map plane, R_{near} is the distance between SAR and the first pixel of a range line, GR_{map} is the projected length of the ground range GR on the map plane, and i_{near} is the incidence angle at the first pixel of a range line. Fig. 1 depicts the calculation, where E is the Earth's radius, GR is the ground range on the Earth's ellipsoid, and α is the angle used in the projection of the ground range to the map plane.

The advantage in correcting the Earth's curvature is that, subsequently, it is possible to directly use ground control in the local coordinate system without worrying about data and transformations between the map and geocentric Cartesian coordinate systems. However, the consideration of the Earth's rotation and, therefore, the modeling of the sensor trajectory in a local coordinate system may not be as accurate as in the geocentric system.

B. SAR Geocoding Procedure

The proposed geocoding procedure consists of the following steps, although some operations can be carried out in different order.

1) Import a SAR image and its auxiliary information (i.e., the ground range pixel size, the time per a range line, the incidence angle at the first pixel of a range line, and the distance from the SAR to the first pixel of a range line).

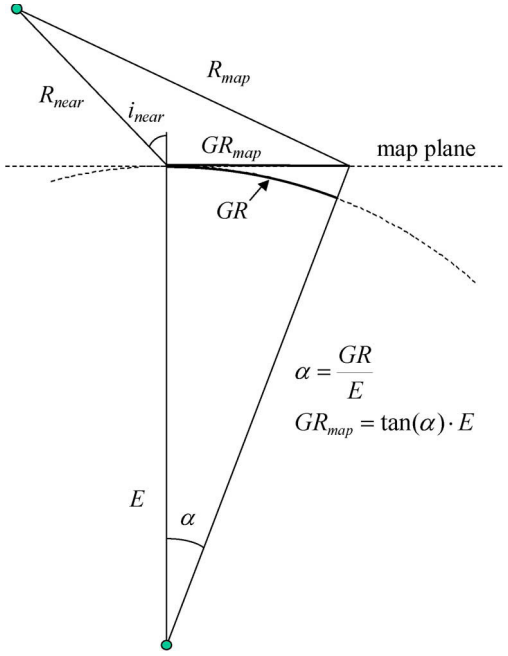

Fig. 1. Correction of SAR ground range values to the map plane.

2) Calculate initial values for the parameters of the affine or the projective transformation model. For example, corners of the SAR image or few GCPs could be used.
3) Import the digital vector map (ArcInfo generate format files). Because maps are 2-D data, the elevations of the control features are acquired from the digital elevation model.
4) The vector map is automatically projected on the SAR image using the affine (or projective) transformation model. The accuracy of the geocoding can be observed directly on the computer monitor.
5) Adjust the input parameters and launch the procedure of automatic GCL localization to produce GCPs.
6) Calculate new values for the transformation parameters using the GCPs and the least squares adjustment. The locations of the GCLs on the SAR image are updated. At this point, it is also possible to alternate between different transformation models to examine their effect on the geocoding accuracy.
7) Repeat steps 5–6 until the geocoding accuracy is satisfactory. Checkpoints may also be used in the accuracy assessment.
8) Finally, it is possible to resample the SAR image to the map coordinate system (also known as orthorectification).

The software for the proposed automatic SAR geocoding procedure can be used in Microsoft Windows. The visible part of the software is the graphical user interface, where both the SAR image and the digital vector map are displayed. The user interface also includes basic tools to adjust the input parameters of the automatic procedure, select the transformation model, and execute the basic import and export operations.

C. Automatic GCL Localization

In the presented geocoding procedure, the goal is to automatically produce GCP measurements, which are then used to solve the unknown parameters of the selected sensor model (i.e., affine, projective, or rigorous SAR sensor model). The most important characteristic is that point features are not used as ground control. However, the heart of the automatic procedure is the edge detection of 3-D GCLs that are projected on the SAR image using the initial or current transformation parameters. The projected GCLs are perpendicularly scanned by moving the scan line between the endpoints of the GCL. The idea of the scan line technique is presented in more detail in [15]. In the case of SAR images, the edge detection algorithm is adjusted to locate the step type of edges and cope with the speckle. The edge detection method and the creation of the virtual GCP are shown in Fig. 2.

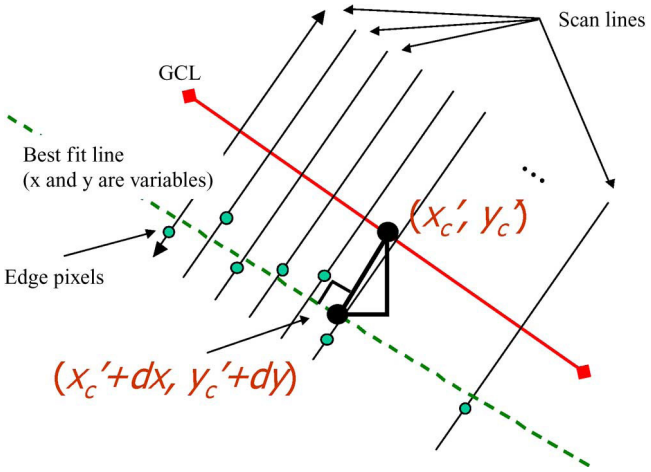

Fig. 2. Automatic localization of GCL from the SAR image.

The edge detection process produces a set of candidate edge pixels, which are assumed to represent the GCL on the image. Then, the best fit line is calculated for the edge pixels, and a virtual GCP is created to the shifted location $(x_c' + dx, y_c' + dy)$ of the center point of the projected GCL (x_c', y_c'). Four examples of the edge detection using Radarsat-1 SAR images are shown in Fig. 3.

As can be seen in Fig. 3, edges are usually detected consistently in good situations. Problems occur in cases where edges are blurry or GCLs are located very closely to each other. However, using a goodness-of-fit value of [0, 1], which describes the linearity of the detected edge pixels, the majority of the problematic edges can be eliminated. The use of a lower threshold value not only produces more successful GCL detections, but also increases the probability of having erroneously detected edges.

A drawback in this procedure is that the virtual GCPs and their corresponding image coordinates contain information about the displacement of the SAR image and the vector map only in the direction, which is perpendicular to the GCL. Therefore, geocoding should always be carried out iteratively by minimizing the displacements.

III. Experiments and Results

The automatic SAR geocoding procedure was tested using three SAR images, which are listed in Table I. The test area is located in southern Finland, where the terrain topography

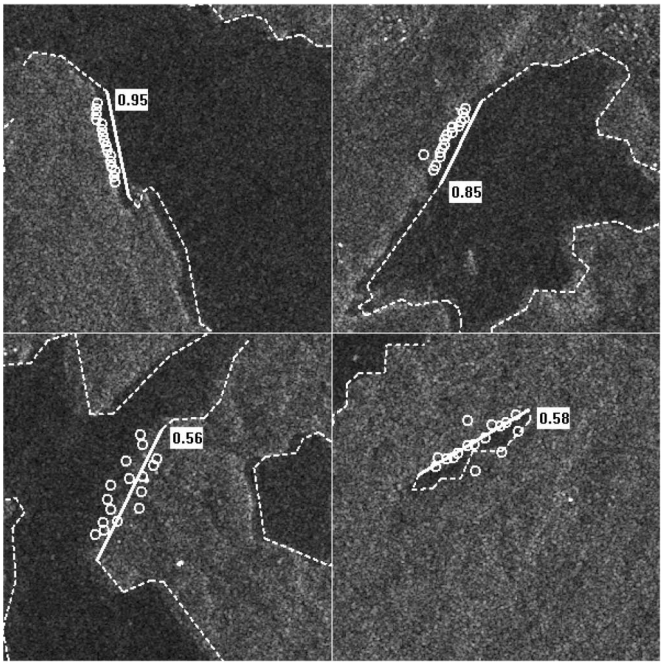

Fig. 3. Examples of edge detection on SAR images.

TABLE I
SAR IMAGES USED IN EXPERIMENTS

Satellite	Scene size (km)	Date	Orbit	Ground range pixel size / Nominal resolution (m)	Incidence angle at first pixel of range line (°)
Radarsat-1	50×50	2 March 2001	Desc.	6.25 / 8.0	36.8
ERS-1	100×100	9 September 1995	Desc.	12.5 / 25.0	19.5
Envisat	110×83	27 February 2003	Desc.	12.5/ 30.0	25.8

is undulating. The elevation values vary from 0 (sea level) to approximately 100 m above the sea level.

First, a few GCPs were roughly measured manually to obtain the initial values for the affine transformation parameters. Next, the automatic GCL localization procedure was carried out (a threshold value of 0.8 was used for goodness of fit). The vector map that was used in the experiments consisted of water body boundaries, which were extracted from the Landsat satellite image. The positional accuracy of the original Landsat image is unknown, but it can be expected to be on the order of a few tens of meters. A digital topographical map derived from aerial images would have been preferred, but such a map was not available in this study. The elevation information for the GCLs was extracted from the digital elevation model of the National Land Survey of Finland. Examples of automatically detected GCLs are presented in Fig. 4. Using a personal computer with 1 GB of physical memory and a 2-GHz processor, edge detection lasts from a few seconds to even tens of minutes, depending on the number of applied GCLs.

After automatic GCL localization, the resulting virtual GCPs were used to solve the parameters of each transformation model. In the case of second- and third-order trajectory polynomials, the coefficients of the one lower polynomial were used as initial values (in fact, the calculation would not be stable otherwise).

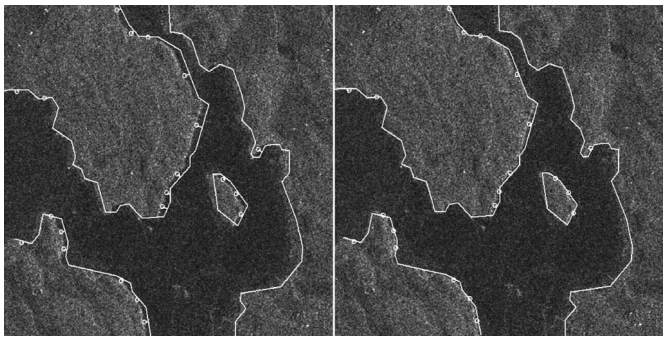

Fig. 4. (Left) Before the automatic geocoding procedure. (Right) After the automatic geocoding procedure.

TABLE II
ESTIMATED GEOCODING ACCURACIES (AFF: AFFINE TRANSFORMATION; PRO: PROJECTIVE TRANSFORMATION; SAR1: SAR SENSOR MODEL WITH THE FIRST-ORDER TRAJECTORY POLYNOMIAL; SAR2 AND SAR3 USE SECOND- AND THIRD-ORDER POLYNOMIALS, RESPECTIVELY)

Satellite --model	Checkpoint RMSE x (pixels)	Checkpoint RMSE y (pixels)	Number of checkpoints	Number of virtual GCPs (detected)
Radarsat-1				
--AFF	4.32	2.47	36	781 (786)
--PRO	4.06	1.87	36	781 (786)
--SAR1	1.81	2.20	36	775 (786)
--SAR2 (*1)	1.77	2.12	36	775
--SAR3 (*2)	1.73	2.16	36	775
ERS-1				
--AFF	3.31	1.59	33	2118 (2184)
--PRO	3.31	1.52	33	2119 (2184)
--SAR1	1.71	1.24	33	2150 (2184)
--SAR2 (*1)	1.67	1.02	33	2150
--SAR3 (*2)	1.69	1.32	33	2150
Envisat				
--AFF	2.41	2.32	34	2161 (2199)
--PRO	2.43	2.17	34	2162 (2199)
--SAR1	1.96	2.34	34	2168 (2199)
--SAR2 (*1)	1.95	1.65	34	2168
--SAR3 (*2)	2.20	1.97	34	2168

*1 = SAR1 polynomial coefficients were used as initial values
*2 = SAR2 polynomial coefficients were used as initial values

Then, the automatic GCL localization procedure was again carried to enhance the accuracy of the geocoding iteratively. After three to five iterations (depending on the test image), the accuracy was acceptable, and the geocoding process was completed.

The accuracies of the final geocoding parameters were analyzed with manually digitized checkpoints, whose positional accuracy should be better than two pixels on the SAR images. The root mean square error (RMSE) was calculated for the differences between the measured and projected image coordinates of the checkpoints. The RMSE values for the different models and the numbers of used virtual GCPs and checkpoints are represented in Table II.

Because the calculation of the transformation parameters also included outlier removal, the number of detected virtual GCPs was higher than the number of virtual GCPs that were actually used in the geocoding. Outlier removal was not used in

the case of second- and third-order polynomials because of their sensitivity to the errors. As can be seen in Table II, the accuracy of the rigorous SAR sensor model is better for all test images. Obviously, affine and projective transformations were not able to correct distortions due to the terrain topography. Hence, the accuracy in the x-direction (range) was worse than that in the y-direction. The projective model appears to be somewhat better than affine, but the reason is that there are more parameters in the projective model, which is therefore able to better adjust to the errors in the ground control. The rigorous SAR sensor model with the first- and second-order polynomials provided the best accuracies. It is noticeable that, in some cases, the accuracies for the third-order polynomial were slightly poorer than those for the lower order polynomials. Probably, the reason is that the errors in the automatically located GCLs can cause some unwanted distortions.

IV. Conclusion

This letter has presented a possible approach to automate the SAR geocoding. According to the experiments, the procedure appeared to be both fast and reliable. The heart of the proposed procedure is automatic GCL localization, which typically lasts only a few seconds, after which the resulting geocoding accuracy can be directly observed from the computer monitor. Therefore, the geocoding accuracy can be easily enhanced iteratively, which is relatively effortless when compared to the completely manual geocoding. The accuracies of the resulting geocoded test SAR images were on the order of two pixels, which is quite close to the nominal spatial resolutions of the used images. However, the initial values of the transformation parameters have to be relatively good prior to the automatic procedure. If the projected GCLs are very far away from the linear features on the image, then the result will be completely erroneous. According to the experiments, the procedure was able to converge to good solution if the initial values were within the accuracy of a few tens of pixels. The accuracy requirement for the initial values depends on the target area and the density and distribution of the applied GCLs.

The applied vector map plays an important role in the proposed procedure. Obviously, the vector map should consist of such line features that are visible on the SAR images. For example, in this study, the boundaries of water bodies were used, because they were easily detected from the test SAR images. In some cases, roads and boundaries of the land-use classes might also be applicable, as long as it is possible to automatically detect them on the images.

Acknowledgment

The author would like to thank Prof. J. Hyyppä for his support, supervision, and precious comments. ERS-1 and Envisat images were provided by the European Space Agency. The Radarsat-1 image was distributed by Radarsat International, TSS, and Novosat Ltd.

References

[1] B. Zitová and J. Flusser, "Image registration methods: A survey," *Image Vis. Comput.*, vol. 21, no. 11, pp. 977–1000, Oct. 2003.
[2] T. Toutin, "Review article: Geometric processing of remote sensing images: Models, algorithms and methods," *Int. J. Remote Sens.*, vol. 25, no. 10, pp. 1893–1924, May 2004.
[3] J. Curlander, "Location of space borne SAR imagery," *IEEE Trans. Geosci. Remote Sens.*, vol. GRS-20, no. 3, pp. 359–364, Jul. 1982.
[4] C. M. Huang, J. K. Guo, Z. Zhao, Z. Xiao, C. P. Qiu, L. Pang, and Z. Y. Wang, "DEM generation from stereo SAR images based on polynomial rectification and height displacement," in *Proc. IGARSS*, Sep. 2004, vol. 6, pp. 4227–4230.
[5] I. Lauknes and E. Malnes, "Automatical geocoding of SAR products," in *Proc. Envisat & ERS Symp.*, Salzburg, Austria, Sep. 2004.
[6] S. E. Masry, "Digital mapping using entities: A new concept," *Photogramm. Eng. Remote Sens.*, vol. 48, no. 11, pp. 1561–1599, Nov. 1981.
[7] Y. Liu and T. S. Huang, "Estimation of rigid body motion using straight-line correspondences," *Comput. Vis. Graph. Image Process.*, vol. 43, no. 1, pp. 37–52, Jul. 1988.
[8] O. Hellwich, H. Mayer, and G. Winkler, "Detection of lines in synthetic aperture radar (SAR) scenes," in *Proc. Int. Archives Photogramm. Remote Sens.*, Vienna, Austria, 1996, pp. 312–320.
[9] F. Tupin, H. Maitre, J.-F. Mangin, J.-M. Nicolas, and E. Pechersky, "Detection of linear features in SAR images: Application to road network extraction," *IEEE Trans. Geosci. Remote Sens.*, vol. 36, no. 2, pp. 434–453, Mar. 1998.
[10] S. Growe and R. Tonjes, "A knowledge based approach to automatic image registration," in *Proc. Int. Conf. Image Process.*, Oct. 1997, vol. 3, pp. 228–231.
[11] P. Dare and I. Dowman, "An improved model for automatic feature-based registration of SAR and SPOT images," *ISPRS J. Photogramm. Remote Sens.*, vol. 56, no. 1, pp. 13–28, Jun. 2001.
[12] A. F. Habib and R. I. Alruzouq, "Line-based modified iterated Hough transform for automatic registration of multi-source imagery," *Photogramm. Rec.*, vol. 19, no. 105, pp. 5–21, Mar. 2004.
[13] T. Schenk, "From point-based to feature-based aerial triangulation," *ISPRS J. Photogramm. Remote Sens.*, vol. 58, no. 5/6, pp. 315–329, Jul. 2004.
[14] G. Schreier, *SAR Geocoding: Data and Systems*. Karlsruhe, Germany: Wichmann Verlag, 1993.
[15] M. Karjalainen, J. Hyyppä, and R. Kuittinen, "Determination of exterior orientation using linear features from vector maps," *Photogramm. Rec.*, vol. 21, no. 116, pp. 329–341, Dec. 2006.